Novel Azapeptide Inhibitors of Hepatitis C Virus Serine Protease

Murray D. Bailey,* Ted Halmos, Nathalie Goudreau, Ewen Lescop, and Montse Llinàs-Brunet

Boehringer Ingelheim (Canada) Ltd. Research and Development, 2100 Cunard Street, Laval, Quebec (Canada) H7S 2G5

Received February 16, 2004

Azapeptides are known inhibitors of several serine and cysteine proteases. In seeking different classes of inhibitors for the HCV serine protease, a series of novel azapeptide-based inhibitors were investigated which incorporated noncleavable P1/P1′ aza-amino acyl residues. Extensive SAR studies around the P1/P1′ aza-amino acyl fragment resulted in the identification of potent and selective inhibitors. Using NMR studies, we have shown that this series of inhibitors bind in a noncovalent competitive fashion to the NS3 protease active site. The bound conformation of one of these new azapeptide-based inhibitors was determined using the transfer NOE technique. Incorporation of these new aza-amino acyl functionalities in the P1 position provided a handle to probe for new interactions in the S′ region of the enzyme.

Introduction

The hepatitis C virus (HCV) is the major agent responsible for non-A and non-B viral hepatitis worldwide. This viral infection is the leading cause of chronic hepatitis, liver cirrhosis, and hepatocellular carcinoma.[1] The World Health Organization estimates that about 200 million people are infected with this virus worldwide.[2] The HCV RNA genome encodes a single polyprotein precursor of about 3000 amino acids which is proteolytically processed into four structural and six nonstructural (NS) proteins. One of the most studied targets for antiviral therapy against HCV is the virally encoded NS3 serine protease.[3] Recently this target has led to the first reported protease inhibitor to have entered clinical trials, BILN 2061.[4a,b] The NS3 protease has been established as a chymotrypsin/trypsin-like serine protease as shown by structural determination.[5] The protease domain is located at the N-terminal portion of the NS3 protein and is responsible for the proteolytic cleavage of the nonstructural proteins found downstream from it, namely the NS3/NS4A, NS4A/NS4B, NS4B/NS5A, and NS5A/NS5B junctions.[6] It has also been shown that the activity of the NS3 protease is enhanced by the NS4A protein which is an essential cofactor required for polyprotein maturation.[7] We have previously reported our findings that the NS3 protease complexed with an NS4A cofactor peptide is inhibited by the N-terminal cleavage product derived from a modified NS5A/5B peptide substrate.[8] This unusual N-terminal cleavage product inhibition has also been observed with substrates corresponding to the NS4A−NS4B and NS4B−NS5A cleavage sites.[9] Early work from our group made use of hexapeptide Ac-DDIVPC-OH (a modified N-terminal cleavage product from NS5A/5B) as our original lead (IC_{50} = 43 μM). We reported that the P1 cysteine residue which is found in three of the natural cleavage sites of the substrate could be replaced by lipophilic amino acids but not without a loss in potency.[10] In particular, a linear three-carbon chain (norvaline) proved to be an acceptable replacement for the cysteine residue with a 5-fold loss in potency but chemically more stable. We have also reported that, in general, replacement of the P1 terminal carboxylic acid by activated carbonyl functionalities (α-ketoamides or fluorinated ketones) did not produce any substantial increase in potency but did in turn impart a loss in specificity against other serine proteases.[10,11] This unusual characteristic of the HCV serine protease have encouraged us to explore other nonacylating functionalities at the P1 position.

Inhibitor Design. In our continuing efforts to discover new classes of inhibitors of the HCV NS3 serine protease, a strategy which avoided the use of traditional electrophilic carbonyl groups in the P1 position was investigated. In addition to C-terminal carboxylic acids, one approach we considered consisted of substitution of the α-carbon atom of the P1 amino acid residue by a trivalent nitrogen atom to yield an azapeptide P1 residue. This strategy seemed particularly appealing since it has been demonstrated that this replacement largely preserves the original peptide conformation in the resulting biomimetic peptide.[12] Moreover, the incorporation of a central P1 aza-amino acyl moiety would fulfill a number of objectives: (1) allow exploration of the S′ region of the enzyme to identify new binding interactions, (2) remove the C-terminal charged residue, and (3) reduce the peptidic character of the inhibitors since azapeptides are known to be metabolically more stable to enzymatic degradation[13] than their amino acid counterparts.

Azapeptide-based inhibitors have been investigated for several serine proteases such as the porcine pancreatic[14,15] and human leukocyte elastases,[15,16] α-chymotrypsin,[17,18] subtilisins,[18] and human leukocyte cathepsin G.[18] We have reported on the use of azapeptides as inhibitors of the HCV serine protease.[19] Recently, others have reported on the use of azapeptides as inhibitors of HCV serine protease which involved the introduction of a variety of groups in the P1′ position with binding affinities varying by >500-fold depending on the nature of the group.[20] One observation was that the potencies of these compounds correlated with the leaving group ability of the P1′ functionality. Regardless

* To whom correspondence should be addressed. E-mail: mbailey@lav.boehringer-ingelheim.com.

10.1021/jm049864b CCC: $27.50
Published on Web 06/17/2004

Scheme 1. Final Assembly and Deprotection[a]

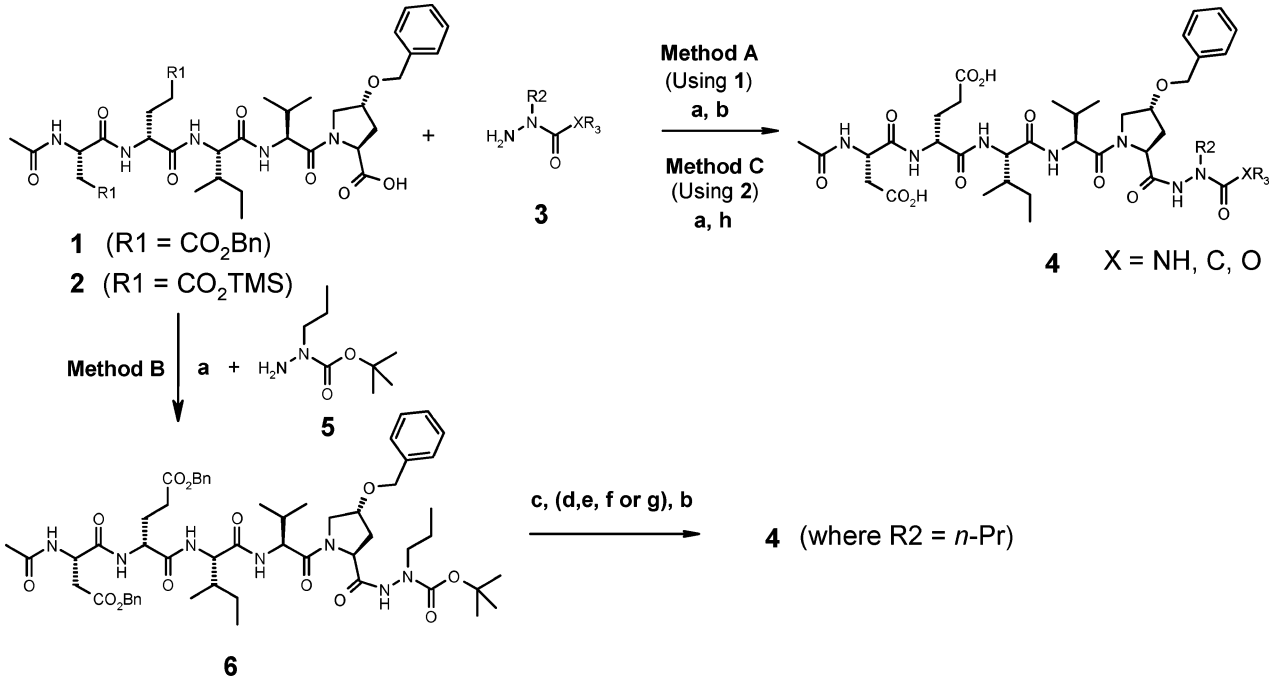

[a] Reaction conditions: (a) TBTU, *i*-Pr_2NEt, DMF, rt; (b) 10% Pd/C, EtOH, NH_4OAc;(c) 4 N HCl/dioxane, 30 min, rt; (d) isocyanate, NEt_3, THF, 0 °C; (e) carboxylic acid, TBTU, DIPEA, DMF; (f) chloroformate, NEt_3, THF; (g) isothiocyanate, NEt_3, THF, 0 °C; (h) neat TFA, 1.5 h.

of this, these azapeptides consistently seemed to display competitive inhibition kinetics.[20] In general however, the approach of introducing labile groups in the P1′ position in azapeptide analogues have resulted in the inhibition through the acylation of the active site serine residue (the active site serine residue nucleophilically attacks the activated carbonyl and forms an acyl-enzyme).[16] The acyl-enzyme intermediate has also been shown to be quite stable, resulting in a slow deacylation rate.[16] In contrast, we envisioned the possibility of introducing a noncleavable aza-amino acyl fragment in the P1−P1′ position to generate noncovalent, reversible inhibitors. In this report we describe extensive SAR studies around the P1 azapeptide moiety of these inhibitors which have lead to the discovery of new interactions within the S1′ region of the enzyme and the generation of a novel series of azapeptide-based inhibitors of the HCV serine protease.[21]

Chemistry. The synthesis of the various aza-amino acyl fragments and the final inhibitors are described in Schemes 1−3. The final assembly and deprotection routes to the azapeptide inhibitors followed a straightforward and divergent approach as outlined in Scheme 1. Specifically, three assembly methods were used to prepare the azapeptide-based inhibitors. In method A, the aza-amino acyl P1/P1′ unit **3** was coupled to the protected pentapeptide **1** (P6−P2) using standard peptide coupling protocols. Removal of the benzyl ester groups under hydrogenation conditions afforded the final inhibitors **4**. This approach was conveniently used to study various alkyl groups on the central P1 nitrogen atom. To probe the importance of other structural features of the aza-amino acyl fragment in the P1′ position, Method B was followed (Scheme 1). This method installs a common carbazate fragment **5** with a defined *N*-alkyl group to pentapeptide **1** to give intermediate **6**. This versatile intermediate is well suited to allow for the exploration of either the P1−P1′ linkage or variations of the P′ group. Derivatization of the carbazate intermediate **6** was conducted by first removal of the *tert*-butyl carbamate group, followed by subsequent treatment with a variety of reactive electrophiles. Final deprotection as before yielded the azapeptide inhibitors **4**. These two strategies proved to be both practical and expedient for SAR studies when X = C or NH. A modification of Method A was utilized to prepare the benzyl carbamate analogues (X = O) since hydrogenation is incompatible with this group. Method C utilized 2-(trimethylsilyl)ethyl ester groups to protect the P5 and P6 acid functionalities in the pentapeptide fragment **2**. This protecting group is extremely useful when using Boc-protected peptides since it survives anhydrous HCl conditions used to cleave *tert*-butyl carbamate groups, while being readily liberated with either TFA or *n*-BuNF treatment.[22] The preparation of the aza-amino acyl fragments **3** used in Methods A and C followed analogous protocols as previously reported by others[23] (Scheme 2). Starting with commercially available *tert*-butylhydrazine **7**, the desired P1 side chains were readily incorporated via a two-step sequence by first formation of hydrazones **8a**−**g** with the appropriate aldehyde or ketone followed by subsequent reduction with DIBAL to produce the *N*-alkyl hydrazines **9a**−**g**. The various P1/P1′ linkages were then obtained by condensation of **9a**−**g** with isocyanates, chloroformates, carboxylic acids, carbamoyl chlorides, or thioisocyanates as shown in Scheme 2 to give the corresponding $C(O)NHR_3$ (**10a**−**g**), C(O)OBn (**11b**), $C(O)CH_2CH_2Ph$ (**12b**), C(O)NR′R″ (**13b**, **14b**), or C(S)-NHBn (**15b**) substituted analogues. The *N*-Me and *N*-CH_2CF_3 analogues were prepared from the available *N*-methylhydrazine and 2,2,2-trifluoroethylhydrazine via an analogous sequence. All of the aza-amino acyl intermediates (**10a**−**g**, **11b**, **12b**, **13b**, **14b**, **15b**) were

Scheme 2. Preparation of the Aza P1/P1′ Fragments[a]

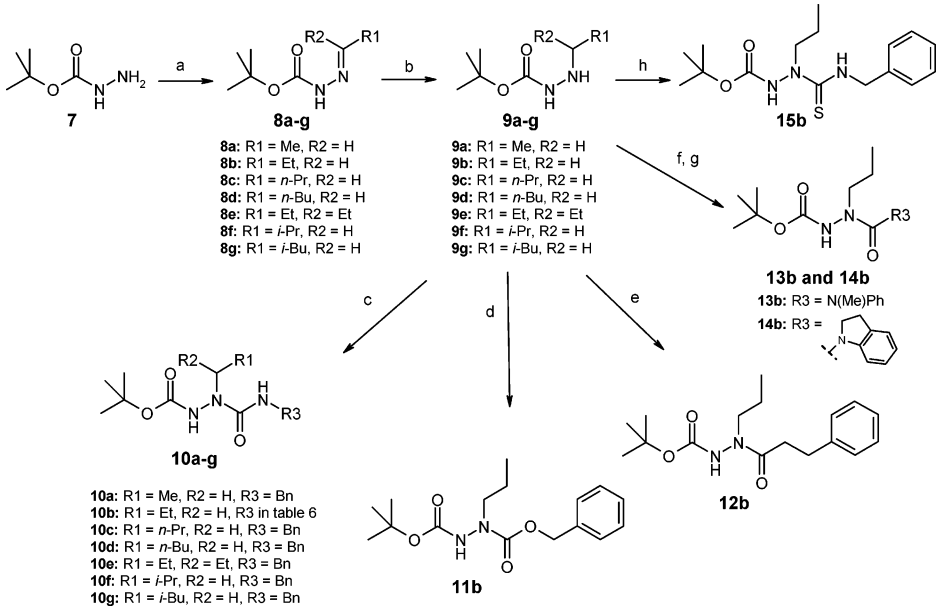

[a] Reaction conditions: aldehyde or ketone, toluene, rt; (b) DIBAL, THF/toluene, −78 °C to rt; (c) R3−N═C═O, *i*-Pr_2NEt, THF, 0 °C to rt; (d) ClCOOBn, *i*-Pr_2NEt, THF, pyridine 0 °C to rt; (e) $PhCH_2CH_2CO_2H$, TBTU, *i*-Pr_2NEt, 0 °C to rt; (f) phosgene/toluene, *i*-Pr_2NEt, THF, 0 °C, 45 min; (g) NH(Me)Ph or indoline, THF, *i*-Pr_2NEt, 0 °C to rt, 16 h; (h) Bn−N═C═S, *i*-Pr_2NEt, 0 °C to rt.

Scheme 3. Alternate Approach for Aza P1/P1′ Fragments[a]

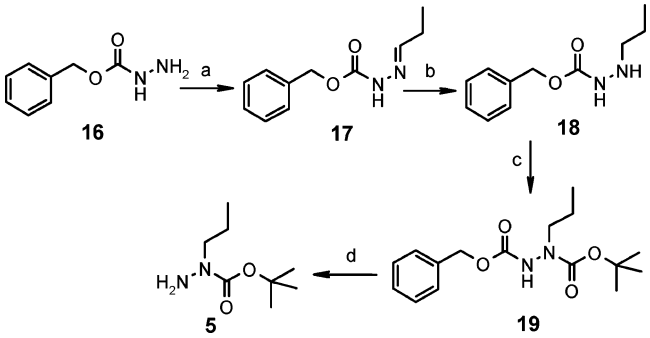

[a] Reaction conditions: (a) propionaldehyde, toluene, rt, NEt_3, THF; (b) DIBAL, THF/toluene, −78 °C to rt; Boc_2O, NEt_3, THF; (d) 10% Pd/C,EtOH, H_2.

subsequently deprotected (removal of the *tert*-butyl carbamate group) before being incorporated into the inhibitor as in Scheme 1, Method A or C. Finally, the preparation of the protected hydrazine **5** used in Method B (Scheme 1) is shown in Scheme 3. Starting from commercially available benzyloxy-carbonyl hydrazine **16**, a reductive alkylation sequence was used to prepare hydrazone **17**, which was subsequently reduced to hydrazine **18** and protected as the *tert*-butyl carbamate derivative **19**. Selective removal of the benzyloxy-carbonyl group afforded hydrazine **5** which was readily incorporated into pentapeptide **1**.

Results and Discussion

It is well-known that the P1 residues of serine protease inhibitors are critical for enzyme specificity and recognition. In an earlier study, we had shown that the naturally occurring P1 cysteine residue could be replaced by the chemically more stable norvaline amino acid. While this replacement is tolerated, a 5-fold loss in potency was realized.[9] Further optimizations to these early hexapeptide analogues have since been described

Table 1. Optimization of Compound **20**

Compound	IC_{50} (μM)
20 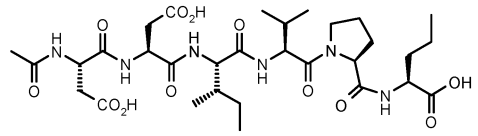	150
21 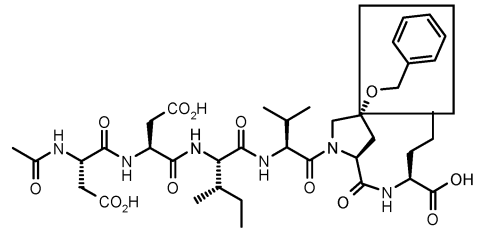	7
22 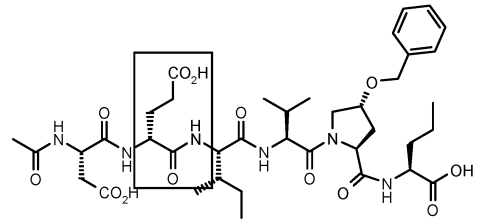	0.60

by us and are shown in Table 1.[11] One of the most important findings was the introduction of substituents on the P2 proline moiety of compound **20**. Incorporation of a (*R*)-benzyloxy group in the 4-position of proline resulted in a 21-fold improvement in potency as illustrated with compound **21**. Further improvement in potency was realized with the incorporation of a D-glutamic acid residue into the P5 position to give peptide **22** with approximately a 10-fold improvement in potency (IC_{50} = 0.60 μM). Having established an acceptable potency with the terminal carboxylic acid series, we then set out to investigate the effects of changes to the P1 residue. The following observations were made (Table 2). As expected, incorporation of the D isomer of norvaline as in compound **23** resulted in a substantial loss in

Table 2. SAR at the P1 Position

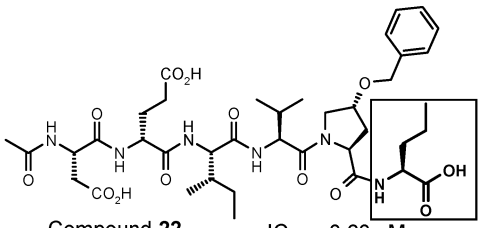

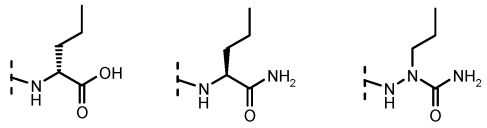

potency (57-fold). More surprisingly however, was the loss in potency realized with the introduction of a terminal amide group of L-norvaline as in compound **24**. Even with the natural amino acid configuration, this simple substitution resulted in greater than a 40-fold loss in potency. Substitution of the α-carbon atom in **24** for a trivalent nitrogen atom afforded the azapeptide-based inhibitor **25**, which was of similar potency to the amino acid analogue **24**. The acceptability of this backbone atom replacement is based on the assumption that the orientation of the *N*-alkyl side chain can adopt the same basic structure as the corresponding peptide, although this has been shown to be structure dependent.[24,25] Other features of the azapeptide-based analogue may also be responsible for maintaining the potency of **25** in relation to amide **24**. It has been shown that the acidity of the P1−NH is enhanced over its amino acid counterpart[14,26] and might improve the hydrogen bonding interaction with the enzyme. As well, the electronic nature of the urea carbonyl in the azapeptide is expected to be different than that of the corresponding amide carbonyl in amide **24**. While azapeptide **25** was substantially less potent than the C-terminal carboxylic acid inhibitor **22** (29-fold less potent), the potential to explore the S′ binding domain encouraged us to investigate this novel series further. Having validated the concept that the P1 amino acid could be replaced by the corresponding aza-amino acyl counterpart, our attention was focused on the introduction of residues into the P′ position. Our objective was to probe the S′ region for new binding interactions necessary to improve the intrinsic potency. A dramatic improvement was observed when hydrophobic residues were incorporated. As shown in Table 3, incorporation of a terminal benzyl group as in compound **26** resulted in a 30-fold improvement in potency over **25**. Interestingly, this more elaborate P1′ residue produced the first azapeptide analogue with equivalent potency to the corresponding terminal acid inhibitor (compound **22)** but without the associated charge. Addition of substituents on the phenyl ring was also well tolerated as shown by the introduction of the piperonylamine group in compound **27**. N-Methylation or rigidification of the terminal amide linkage as in compounds **28** and **29** were, however, found to be detrimental to the potency. Disubstitution on the terminal nitrogen atom likely results in an unfavorable conformational change which is not well suited for the active site.

Table 3. SAR at the P′ Position

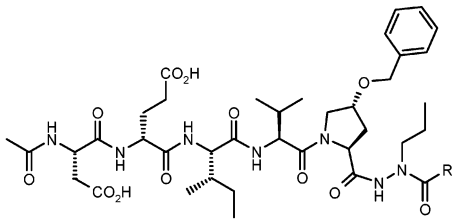

Compound	R	IC_{50} (μM)
25		17.5
26	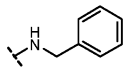	0.59
27	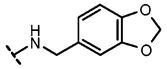	0.50
28	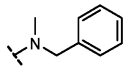	8.4
29	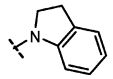	4.4

Table 4. Importance of the P1′-NH and P1-CO Group

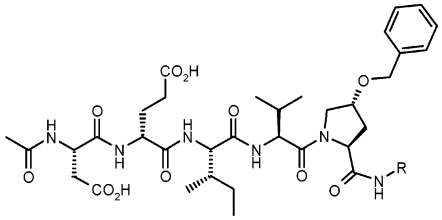

Compound	R	IC_{50} (μM)
26	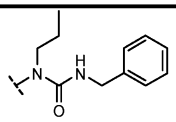	0.59
30	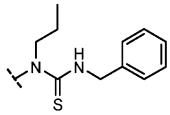	4.2
31	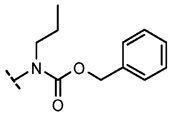	0.80
32	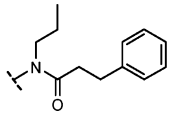	0.71

The importance of the linkage between the P1−P1′ residue was also investigated (Table 4). First, the importance of the P1 carbonyl group was established by the simple substitution of the carbonyl in carbamate **26** by the thiocarbonyl group as in **30** which resulted in greater than a 7-fold drop in potency. The nature of the linking atom between P1−P1′ was shown to have little or no effect on potency. Replacement of the terminal monosubstituted nitrogen atom by either an oxygen (compound **31**) or carbon atom (compound **32**) were equally well tolerated. Analogue **32** is of particular interest since this compound clearly rules out the

Table 5. Effect of A-Branching in the P1′ Position

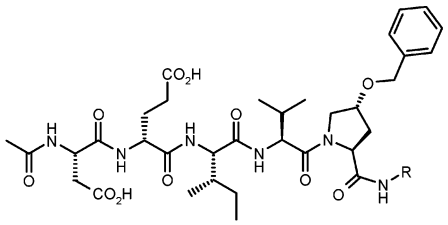

Compound	R	IC_{50} (μM)
26	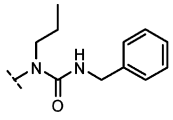	0.59
33	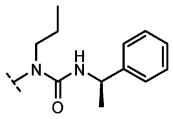	4.3
34	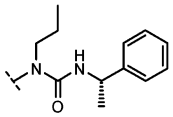	0.078
35	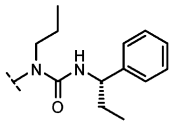	0.44
36	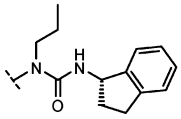	0.10
37	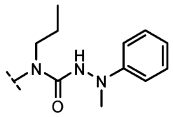	0.48
38	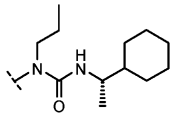	0.42
39	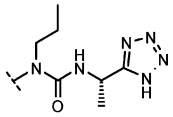	0.86
40	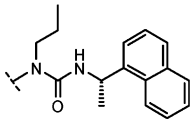	0.49
41	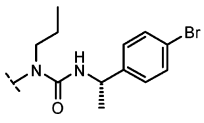	0.072

possibility of having inhibition through the enzyme acylation pathway as described for reactive azapeptides. From this study it appears that while the NH(P1′) is nonessential for potency, the carbonyl (P1) contributes significantly to the activity of these compounds. Having established that a benzyl group in the P′ position was beneficial to potency (Table 3), further modifications were investigated (Table 5). Incorporation of an α-methyl group in the benzylic position with the "R" configuration (compound **33**) resulted in a 7-fold loss in potency. However, substitution with the enantiomeric α-(*S*)-methyl group as in compound **34** resulted in more than a 7-fold improvement in potency relative to **26**. The preference for the (*S*)-methyl group in the P′ region is presumably a result of a beneficial orientation of the aryl group. It is interesting to note that the stereospecificity of the P1′ position as observed here has also been observed for other protease targets.[27] Further investigation into the effect of α substitution revealed that while lengthening of the side chain as in **35** was not well tolerated, rigidification as in **36** was well accepted. Replacement of the α stereocenter by the *N*-methyl phenylhydrazine moiety as in **37** resulted in a compound which loses the beneficial effect of the α-substitution and is similar in potency to **26**. The necessity of the phenyl ring was next examined. Saturation of the aromatic ring as in compound **38** or incorporation of a tetrazole ring as in compound **39** was not beneficial. Increasing the size of the aryl group such as in **40** was also detrimental. It was found, however, that substitution is tolerated in the para position of the phenyl ring as in **41** which was equipotent ($IC_{50} = 0.072\ \mu M$) to compound **34.** From this table, the optimal modifications in the P′ region were found for compound **34** which was over 7-fold more potent than the starting benzyl analogue **26**. It also appears from compound **41** that further modifications are possible on the phenyl ring.

P1 Side Chain Optimization. The replacement of the α-carbon in an amino acid by a trivalent nitrogen atom has a number of consequences. One of these is that the conformation adopted by the aza-amino acid moiety around the α-nitrogen atom can be significantly affected depending on the peptide sequence. While some have considered the conformation somewhere intermediate between the D- or L-amino acid,[13] others have shown that the α-nitrogen atom can be nearly planar.[24] These possible conformational effects around the α-aza-substitution prompted us to investigate whether the *n*-propyl side chain (aza-norvaline) was fully optimal in our case. Three issues were examined, the length of the side chain, the effect of branching, and the effect of fluorine substitution (Table 6). Chain lengths of two, three, or four carbon atoms, as in compounds **43**, **34**, and **44**, were found to be more or less equipotent against the protease. Incorporation of shorter or longer chain lengths as in compounds **42** or **45** were much less favorable, showing that the enzyme requires at least a two- to four-carbon side chain. The effect of branching was also investigated. Branching at various positions along the side chain were not well tolerated (compounds **46**, **47**, **48**), indicating that larger alkyl groups are not well suited for this enzyme. In addition, the introduction of a trifluoromethyl group as in derivative **49** was also found not to be optimal for binding.

Specificity. A number of these azapeptide-based analogues were screened for their activity against other serine or cysteine proteases. In particular, special attention was paid to human leukocyte elastase (HLE) which has a high substrate sequence homology to that of the NS3 protease in the P3 through P1 residues (Table 7). The selectivity between the NS3 serine protease and HLE was found to be dependent on the P1 side chain. The least selective compound was found to be compound **34** having a three-carbon side chain.

Table 6. SAR on the P1 Side Chain

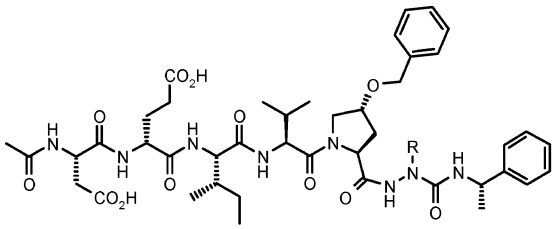

Compound	R	IC_{50} (μM)
42		**0.43**
43		**0.085**
34		**0.078**
44	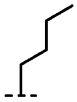	**0.099**
45	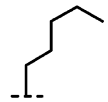	**0.49**
46		**4.1**
47		**2.4**
48	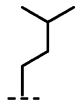	**5.7**
49		**0.34**

This compound exhibited a 65-fold window between IC_{50} values. The most selective inhibitor from this study (compound **44**) exhibited more than a 400-fold window between IC_{50} values and incorporated the slightly longer butyl side chain. This difference in selectivity between **34** and **44** comes about by maintaining the excellent potency level against the HCV serine protease while decreasing the affinity toward the human leukocyte elastase enzyme. The methyl and *n*-pentyl analogues (**42** and **45**) also showed selectivity against HLE but these were also much less potent against the desired HCV serine protease. Additionally, compounds **34**, **42**−**45** were also screened against chymotrypsin and cathepsin B and were shown to be completely selective (>150 μM).

NMR Studies. To get a better understanding of how the azapeptide-based inhibitors bind to the NS3 protease, NMR studies were conducted using compound **25** (Table 3). Unfortunately, the study of our more potent inhibitors which extend into the P1′ region using the transfer-NOE approach was not possible due to the high intrinsic potencies of these compounds and the slow on/off rates. Our initial NMR investigations focused on determining which parts of azapeptide **25** interact with the NS3 protease. This was accomplished using differential line-broadening techniques which we have previously described.[28−30] Figure 1 presents a region of the 1D ^{1}H NMR spectrum of **25** recorded in absence (blue trace) and in the presence (red trace) of the NS3 protease. In the absence of enzyme, the inhibitor has sharp resonance line shapes while in the presence of the NS3 protease specific differential line broadening effects are observed. Indeed, the P1 side chain resonances (γ-CH_3 at 0.88 ppm and β-CH_2 at 1.52 ppm), and the P3 Val and P4 Ile methyl resonances (P3 γ-CH_3 at 0.93 ppm and P4 γ-CH_3 at 0.79 ppm/δ-CH_3 at 0.81 ppm) experience significant line broadening, while no significant change is observed for other resonances such as the P4 Ile β-CH (1.86 ppm) and γ-CH_2 (1.42 ppm) and the P5 D-Glu β-CH_2 (1.93 ppm). The specific nature of these protease-induced perturbations suggests that the segments of **25** which have their resonances affected by the addition of NS3 are likely at or near the binding interface. In a second step, the transfer NOE technique was applied to azapeptide **25** in order to establish the NS3 bound conformation. This technique has previously

Table 7. Comparison between HLE and HCV Protease with Various P1 Residues

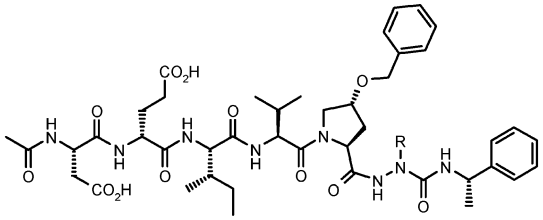

Compound	R	IC_{50} (μM) HLE	IC_{50} (μM) HCV	Δ
42	Me	168	0.43	390
43	Et	21	0.085	247
34	*n*-Pr	5	0.078	65
44	*n*-Bu	41	0.099	414
45	*n*-Pentyl	151	0.49	308

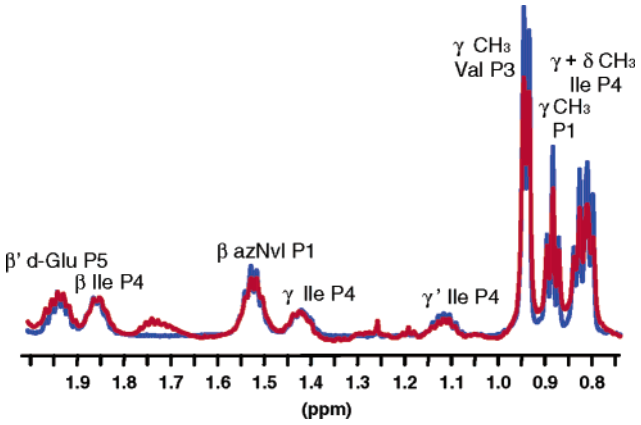

Figure 1. Subregion of ^{1}H spectra of inhibitor **25** recorded in the absence (blue) and in the presence (red) of NS3 protease at an inhibitor-to-protease ratio of 34:1. Upon addition of the protease, significant line broadening was observed for specific resonances.

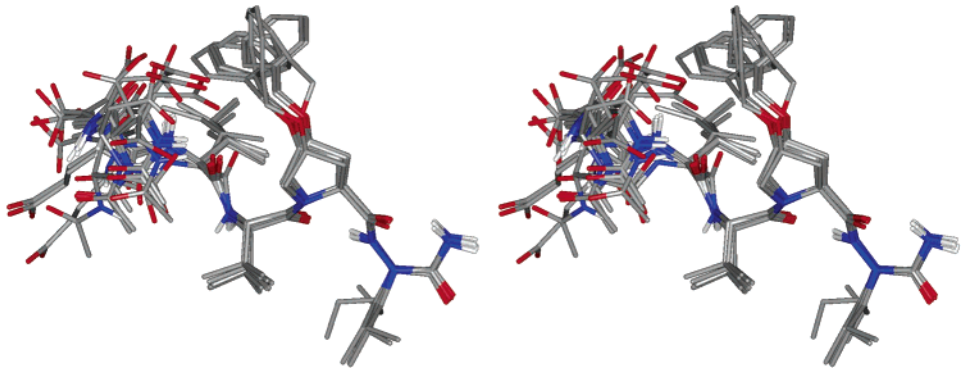

Figure 2. Stereoview of the superposition (P1−P4 backbone atoms only) of the eight best structures generated by restrained simulated annealing and derived from the NMR data of inhibitor **25** when bound to the NS3 protease. The structures are colored by atom type (oxygen is red, nitrogen is blue, carbon is dark gray, and hydrogen is light gray). Most of the hydrogen atoms are not shown.

been successfully used for hexapeptide **22**.[30] Part A of the figure in Supporting Information shows a region of the 2D NOESY spectrum of inhibitor **25** recorded in the absence of the NS3 protease where only a few NOEs are observed as expected for a small molecule of this size. In contrast, the NOESY spectrum of inhibitor **25** recorded after the addition of the NS3 protease (34:1 inhibitor-to-protease ratio) reveals an extensive set of new, negative transferred NOE cross-peaks (part B). The detection of these transferred NOEs also confirms the reversibility and the fast exchange binding of **25** to the NS3 protease. To establish that these transferred NOEs come from the binding of **25** to the enzyme active site, a competition experiment was carried out. In this experiment, a potent covalent and reversible α-keto-amide inhibitor (serine-trap based) (IC_{50} = 0.023 μM) which is known to block the NS3 active site was added to the above azapeptide **25**/NS3 protease sample (at four times the concentration of the enzyme) and a NOESY spectrum was reacquired (part C). The resulting disappearance of the previous set of transferred NOE cross-peaks and the restoration of the spectrum to that of the free inhibitor (part C versus part A) is a clear indication of the displacement of **25** from the NS3 active site by the potent serine-trap-based inhibitor and supports the claim that these compounds are noncovalent competitive inhibitors of the protease.

Having established that the transferred NOE cross-peaks in part B arise from **25** when bound to the active site of the NS3 protease, we then focused our efforts on determining the bound conformational properties of **25**. For this, the distance restraints derived from the volumes of the transferred NOEs cross-peaks were used in a simulated annealing protocol in order to generate an ensemble of bound conformations. Figure 2 displays a stereoview of the final eight low energy, transferred NOE-consistent structures of **25** that are superimposed from P1 to P4. A well defined, extended conformation is clearly evident (from P1−P4) with a root-mean-square deviation for the P1−P4 backbone atoms of 0.21 Å. The side-chain conformations are also rather well defined for most residues with the exception of P5 and P6 residues which show a larger degree of variation due to a smaller number of restraints involving their side chains. Moreover, the P2 and P4 side chains lie close to each other in the bound state as evidenced by the observation of transferred NOEs between the P4 γ-CH_3 and β-CH and the P2 aromatic protons.

Altogether, this NMR study clearly demonstrates that the azapeptide **25** binds to the NS3 protease in an overall extended conformation that is very similar to that of the C-terminal carboxylic acid series of inhibitors such as hexapeptide **22**.[30] In particular the P1 aza-amino acyl group of inhibitor **25** adopts a conformation that is quite comparable to the one adopted by the P1 norvaline residues of hexapeptide **22**. In addition, similar differential line broadening patterns were also observed for both of these P1 residues, therefore corroborating the concept that the P1 amino acid can be replaced by its aza-amino acid counterpart.

Conclusion

We have successfully identified a new series of potent NS3 serine protease inhibitors that incorporate an aza-amino acyl fragment at the P1/P1′ position. While the P1/P1′ NH linkage was found to be nonessential, the P1 carbonyl group was shown to play an important role in binding to the enzyme. The introduction of an α-(*S*)-methyl benzyl group in the P1′ position of the inhibitor was critical for improving potency and presumably helps orient the aryl group into the enzyme. Benzylic residues were found to be the most preferred groups in the S′ region of the enzyme since the larger biaryl substitution resulted in reduced activity. Transferred NOE experiments have shown that compound **25** binds in an extended conformation, similar to that observed for the C-terminal carboxylic acid inhibitor series previously reported. Through NMR displacement studies with the enzyme, this family of azapeptide-based inhibitors were shown to act through a noncovalent competitive mode of inhibition since a potent serine-trap-based inhibitor displaced the azapeptide inhibitor from the active site. The choice of the P1 side chain was very important for providing specificity against other serine proteases. Our best inhibitor in terms of potency and specificity was compound **44**, with an IC_{50} = 0.099 μM against the HCV NS3 serine protease, and a window of greater than 400-fold when counterscreened against human leukocyte elastase. Continued efforts with this inhibitor class would include the further optimization of the P1−P4 residues and reduction in size through truncation studies.

Experimental Section

Chemistry. Unless otherwise noted, materials were obtained from commercial sources and used without further purification. The purity of each inhibitor was determined by

HPLC using two systems. ^{1}H NMR spectra were obtained on a Bruker AMX 400 spectrometer and can be found in the Supporting Information. FAB mass spectra were recorded on an Autospec, VG spectrometer. Column chromatography was performed either on silica gel (10−40 μm or 230−400 mesh ASTM, E. Merck) or by preparative HPLC using a Partisil 10 ODS-3, C18 preparative column (50 cm × 22 mm). Analytical HPLC were carried out on the following systems: System A: Vydac C18, 10 μm analytical column (24 cm × 4.6 mm); mobile phase, acetonitrile/0.06% trifluoroacetic acid (TFA) in water/0.06% TFA; System B: ODS-AQ, Combiscreen, 5 μm analytical column (50 mm × 4.6 mm); mobile phase, acetonitrile/0.06% trifluoroacetic acid in water/0.06% TFA; System C: Symmetry C8, 5 μm analytical column (2.1 × 150 mm); mobile phase, acetonitrile/50mM NaH_2PO_4, pH = 4.4.

General Protocol for the Preparation of Compounds 8a−g. Preparation of *N*′-Propylidenehydrazinecarboxylic Acid *tert*-Butyl Ester 8b. To a solution of Boc-hydrazine **7** (3.0 g, 22.6 mmol) in toluene (42 mL) was added propionaldehyde (1.8 mL, 24.9 mmol). The solution was heated to 50 °C for 1 h and then stirred at RT for 24 h. The mixture was concentrated to give **8b** as a white solid (3.70 g, 95%) which was homogeneous by analytical HPLC (97.5%). MS (FAB) 173.1 (MH^+).

Preparation of *N*′-Ethylidenehydrazinecarboxylic Acid *tert*-Butyl Ester 8a. Obtained from **7** (2.0 g, 12.6 mmol) using the procedure described for **8b** but utilizing acetaldehyde (0.78 mL, 13.9 mmol) afforded **8a** (1.99 g, 100%) as a colorless oil. HPLC homogeneity (99%); MS (FAB) 159 (MH^+).

Preparation of *N*′-Butylidenehydrazinecarboxylic Acid *tert*-Butyl Ester 8c. Obtained from **7** (2.64 g, 20 mmol) using the procedure described for **8b** but utilizing butraldehyde (1.8 mL, 20 mmol) afforded **8c** (2.25 g, 60%) as a white solid after purification by chromatography (SiO_2, 2:1 hexane/EtOAc). HPLC homogeneity (99%); MS (FAB) 187 (MH^+).

Preparation of *N*′-Pentylidenehydrazinecarboxylic Acid *tert*-Butyl Ester 8d.

Obtained from **7** (2.5 g, 18.9 mmol) using the procedure described for **8b** but utilizing *n*-valeraldehyde (2.2 mL, 21 mmol) afforded **8d** (3.78 g, 100%) as a colorless oil. MS (FAB) 201.1 (MH^+). This material was sufficiently clean to be used as is in the next step.

Preparation of *N*′-(1-Ethylpropylidene)hydrazinecarboxylic Acid *tert*-Butyl Ester 8e. Obtained from **7** (2.5 g, 18.9 mmol) using the procedure described for **8b** but utilizing 3-pentanone (3.2 mL, 21 mmol) afforded **8e** (3.5 g, 92%) as a colorless oil. MS (FAB) 201.1 (MH^+).

Preparation of *N*′-[2-Methylpropylidene]hydrazinecarboxylic Acid *tert*-Butyl Ester 8f. Obtained from 7 (2.5 g, 18.9 mmol) using the procedure described for **8b** but utilizing isobutyraldehyde (1.9 mL, 21 mmol) afforded **8f** (3.5 g, 100%) as a colorless oil. MS (FAB) 187.1 (MH^+), 209.1 $(M + Na)^+$.

Preparation of *N*′-[3-Methylbutylidene]hydrazinecarboxylic Acid *tert*-Butyl Ester 8g. Obtained from 7 (2.5 g, 18.9 mmol) using the procedure described for **8b** but utilizing isovaleraldehyde (1.3 mL, 21 mmol) afforded **8g** (3.8 g, 100%) as a colorless oil. MS (FAB) 201.4 (MH^+), 223.3 $(M + Na)^+$.

General Procedure for Preparation of Compounds 9a−g. Preparation of *N*′-Propylhydrazinecarboxylic Acid *tert*-Butyl Ester 9b. To imine **8b** (3.7 g, 21.48 mmol) in THF (80 mL) at −78 °C was added DIBAL (31 mL, 47.25 mmol) as a 1.5 M solution in toluene. The reaction was maintained at −78 °C for 2 h and then −40 °C for 2 h. The mixture was then warmed to RT before Rochelle's salt (aqueous potassium sodium tartrate) solution was added and the reaction mixture stirred at RT overnight. The organic phase was separated and the aqueous phase extracted with Et_2O (2 × 75 mL). The combined organic extracts were washed with brine, dried (Na_2SO_4), filtered, and concentrated in vacuo. Purification by flash chromatography on silica gel gave intermediate **9b** as a colorless oil (3.4 g, 91%). MS (CI−NH_3) 175.2 (MH^+).

Preparation of *N*′-Ethylhydrazinecarboxylic Acid *tert*-Butyl Ester 9a. Obtained from **8a** (2.4 g, 15 mmol) using the procedure described for **9b** afforded **9a** (1.1 g, 46%) as a colorless oil after chromatography (SiO_2, 3:1 hexane/EtOAc). MS (FAB) 182 ($M + Na^+$).

Preparation of *N*′-Butylhydrazinecarboxylic Acid *tert*-Butyl Ester 9c. Obtained from **8c** (2.22 g, 12 mmol) using the procedure described for **9b** afforded **9c** (2.32 g, 100%) as a colorless oil after chromatography (SiO_2, 3:1 hexane/EtOAc). MS (FAB) 187 ($M-H^+$).

Preparation of *N*′-Pentylhydrazinecarboxylic Acid *tert*-Butyl Ester 9d. Obtained from **8d** (2.0 g, 10 mmol) using the procedure described for **9b** afforded **9d** (0.78 g, 38%) as a white solid after chromatography (SiO_2, 3:1 hexane/EtOAc). MS (FAB) 203.1 (MH^+).

Preparation of *N*′-(1-Ethyl-propyl)hydrazinecarboxylic Acid *tert*-Butyl Ester 9e. Obtained from **8e** (3.5 g, 17.5 mmol) using the procedure described for **9b** afforded **9e** (2.17 g, 61%) after chromatography (SiO_2, 3:1 hexane/EtOAc). MS (FAB) 203.1 (MH^+).

Preparation of *N*′-Isobutylhydrazinecarboxylic Acid *tert*-Butyl Ester 9f. Obtained from **8f** (1.26 g, 6.8 mmol) using the procedure described for **9b** afforded **9f** (0.79 g, 62%) as a white solid after chromatography (SiO_2, 3:1 hexane/EtOAc). MS (FAB) 189.1 (MH^+).

Preparation of *N*′-(3-Methyl-butyl)hydrazinecarboxylic Acid *tert*-Butyl Ester 9g. Obtained from **8g** (3.8 g, 18.9 mmol) using the procedure described for **9b** afforded **9g** (2.0 g, 52%) as a white solid after chromatography (SiO_2, 3:1 hexane/EtOAc). MS (FAB) 203.1 (MH^+).

General Preparation of Compounds 10a−g (representative examples). Preparation of (3-*tert*-BSutylcarbonyl-2-propylcarbazoyl)-(*S*)-methylbenzylamine 10b (where R3 = CH(“*S*”-Me)Ph). The hydrazine **9b** (0.20 g, 1.15 mmol) was combined with (*S*)-(−)-1-methylphenyl isocyanate (0.162 g, 1.15 mmol) in CH_2Cl_2 (2.4 mL) with DIPEA (0.44 mL, 2.52 mmol) and stirred at 0 °C for 1 h and then at RT for 3 h. The mixture was concentrated in vacuo to give a white solid which was purified by flash chromatography to give the protected intermediate **10b** (0.25 g, 68%). MS (FAB) 322.3 (MH^+).

Preparation of (3-*tert*-Butylcarbonyl-2-propylcarbazoyl)amine 10b (where R3 = H). To intermediate **9b** (0.20 g, 1.15 mmol) dissolved in dioxane/H_2O (4 mL, 1:1 mix) was added potassium cyanate (0.19 g, 2.3 mmol) portionwise over 30 min followed by 4 N HCl (aq) (0.28 mL, 1.15 mmol). The solution was stirred at RT (16 h) before the volatiles were removed in vacuo and the residue extracted into EtOAc (50 mL), washed sequentially with 10% citric acid and brine. Then the organic phase was dried (Na_2CO_3), filtered, and concentrated before being purified (SiO_2, 7:3 EtOAc/hexane, $R_f = 0.20$) to give **10b** (R1 = H) as a white solid (0.15 g, 60%). MS (FAB) 218.1 (MH^+).

Preparation of (3-*tert*-Butylcarbonyl-2-propylcarbazoyl)benzyl Alcohol 11b. Intermediate **9b** (0.50 g, 2.87 mmol) was dissolved in anhydrous THF (6 mL) and cooled to 0 °C with anhydrous pyridine (0.29 mL, 3.6 mmol). The solution was treated dropwise with benzyl chloroformate (0.42 mL, 2.95 mmol). The mixture was allowed to slowly warm to RT and stirred 16 h before being diluted with EtOAc (50 mL) and washed with brine. After drying (Na_2SO_4), the material was purified (SiO_2, 4:1 hexane/EtOAc) to give the precursor to **11b** as a white solid (0.80 g, 90%). MS (FAB) 309 (MH^+), 209 $(M - Boc)^+$.

Preparation of *N*′-(3-Phenyl-propionyl)-*N*′-propylhydrazinecarboxylic Acid *tert*-Butyl Ester 12b. To intermediate **9b** (0.20 g, 1.15 mmol) were added hydrocinnamic acid (0.19 g, 1.26 mmol), TBTU (0.40 g, 1.26 mmol), and DIPEA (0.44 mL, 2.53 mmol) in DMF (5 mL) at RT. The coupling reaction was left 16 h before the solvent was removed in vacuo and the product purified (SiO_2, 3:1 hexane/EtOAc) to give the Boc intermediate **12b** as a white solid (0.29 g, 81%). MS (FAB) 307 (MH^+), 207 $(M - Boc)^+$; HPLC homogeneity (system A; 95.5%).

Preparation of (3-*tert*-Butylcarbonyl-2-propylcarbazoyl)-*N*-methylaniline 13b. To a solution of phosgene in toluene (1.93M, 5.1 mL, 9.9 mmol) in dry THF (5 mL) at 0 °C was added a solution of intermediate **9b** (0.43 g, 2.47 mmol)

and diisopropylethylamine (0.94 mL, 5.42 mmol) in THF (5 mL) over 15 min. The mixture was stirred at 0 °C for 30 min before the excess phosgene and solvents were removed in vacuo. The residue was redissolved in THF (5 mL) with DIPEA (0.94 mL, 5.42 mmol) and cooled to 0 °C before a solution of *N*-methylbenzylamine (0.32 mL, 2.47 mmol) with DIPEA (0.94 mL, 5.42 mmol) was added all at once. The reaction was maintained at 0 °C (1 h) and then warmed to RT (16 h). The mixture was poured into EtOAc (100 mL) and washed sequentially with HCl (1 N), sat. $NaHCO_3$, and brine before being dried ($MgSO_4$), filtered, and concentrated. The product was purified by flash chromatography (SiO_2, 2:1 hexane/EtOAc) to afford **13b** as a white solid (0.485 g, 64%). MS (FAB) 322.1 (MH^+).

Preparation of (3-*tert*-Butylcarbonyl-2-propylcarbazoyl)indoline 14b. Following the same protocol as **13b** except using indoline as the amine, **9b** (0.43 g, 2.47 mmol) was converted into compound **14b** (0.56 g, 74%) as a white solid. MS (FAB) 320.1 (MH^+), 342.1 ($M + Na)^+$.

Preparation of (3-*tert*-Butylcarbonyl-2-propylthiocarbazoyl)benzylamine 15b. To intermediate **9b** (16.4 mg, 0.094 mmol) under an inert atmosphere in dry THF (4 mL) at 0 °C was added benzyl isothiocyanate (14 mg, 0.094 mmol) containing DIPEA (36 uL, 0.21 mmol) in THF (2 mL). The mixture was stirred at 0 °C for 1 h and then at RT (16 h). The mixture was partitioned between EtOAc and brine and then washed with 1 N HCl (aq), sat. $NaHCO_3$, and brine. The organic phase was dried ($MgSO_4$), filtered, and concentrated before being purified by chromatography (SiO_2, 2/1 hexane/EtOAc) to give **15b** (17 mg, 56%). MS (electrospray) 346 ($M + Na)^+$. Used as such to prepare the final inhibitor according to Scheme 1.

Preparation of *N*-Propylhydrazinecarboxylic Acid *tert*-Butyl Ester 5. Commercially available benzyl carbazate **16** (12.5 g, 75.3 mmol) in toluene (140 mL) was treated with propionaldehyde (6.0 mL, 83.2 mmol) and heated at 60 °C for 2 h. The solution was cooled and left at RT (16 h). The volatiles were removed in vacuo to afford the Schiff base **17** as a white solid (19.5 g). Part of **17** (10 g, 48.5 mmol) was dissolved in THF (180 mL) and then cooled to −78 °C before DIBAL in toluene (1.5 M, 47 mL, 70.5 mmol) was added from a dropping funnel over 30 min. The solution was stirred an additional 2 h before warming to −40 °C for 2 h. To the solution at −10 °C was added diethyl ether (180 mL) followed by dropwise addition of Rochelle's salt solution (70 mL). The mixture was stirred at RT (16 h), and the solvents were removed. The residue was extracted with diethyl ether (3 × 150 mL), and the combined extracts were washed with sat. brine, dried (Na_2SO_4), filtered, and concentrated to give hydrazine **18** (9.5 g, 94%) as a colorless oil. Hydrazine **18** (5.0 g, 24 mmol) was dissolved in dioxane (20 mL) and added to a solution of 2 N NaOH (13.2 mL, 26.4 mmol) containing di-*tert*-butyl dicarbonate (5.2 g, 24 mmol) with stirring at RT (16 h). The mixture was diluted with EtOAc (200 mL) and washed with water (2 × 200 mL) and brine (1 × 100 mL). The extract was dried (Na_2SO_4), filtered, and concentrated before being purified (SiO_2, 3/1 hexane/EtOAc) to afford compound **19** as a white solid (1.78 g). Finally, removal of the Cbz group was accomplished by dissolving **19** (640 mg, 2.07 mmol) in ethanol with 10% Pd/C (63 mg) under a balloon atmosphere of hydrogen (16 h). The vessel was evacuated and the catalyst filtered off using Celite as a filter aid. Concentration in vacuo gave the desired Boc protected hydrazine **5** (344 mg, 95%) as a colorless liquid. MS (FAB) 175 (MH^+), 197 ($M + Na)^+$.

General Procedure for Preparation of Inhibitors According to Scheme 1 (Method B): Preparation of 38 (Method B). To pentapeptide **1** (1.75 g, 1.95 mmol) in DMF (20 mL) with the Boc-protected hydrazine **5** (0.34 g, 1.95 mmol) and *O*-(7-azabenzotriazol-1-yl)hexafluorophosphate (HATU) (1.26 g, 2.53 mmol) was added DIPEA (1.36 mL, 7.8 mmol). The reaction was allowed to stir at RT (16 h) before being concentrated in vacuo and purified (SiO_2, neat EtOAc) to afford the fully protected peptide **5** (1.4 g, 67%). Following this, peptide **6** (0.15 g, 0.14 mmol) was treated with 4 N HCl/dioxane (3 mL, 30 min, RT) and concentrated to dryness to give the corresponding hydrazinyl HCl salt in quantitative yield. In a separate operation, to a solution of phosgene/toluene (1.93 M, 0.3 mL, 0.57 mmol) in dry THF (2 mL) with DIPEA (59 μL, 0.46 mmol) at 0 °C was added (*S*)-(+)-1-cyclohexylethylamine (21 μL, 0.142 mmol) over 15 min. After being stirred at 0 °C for 30 min, the solvents were removed in vacuo and subsequently redissolved in THF (2 mL) with DIPEA (59 μL, 0.46 mmol). This solution was added to the above-mentioned hydrazinyl HCl salt (dissolved in 2 mL of THF containing 59 μL of DIPEA) at 0 °C and stirred for 1 h and then at RT (16 h). The mixture was concentrated to dryness and dissolved into EtOAc (75 mL) before being washed with 1 N HCl (aq) and brine. The organic phase was dried (Na_2SO_4), filtered, and concentrated to give a pale yellow solid (0.12 g, 0.11 mmol). This crude material was finally deprotected in EtOH (9 mL) with ammonium acetate (12 mg, 0.17 mmol) being added. This mixture was treated with 10% Pd/C (12 mg) and hydrogenated under an atmosphere of H_2 (1 atm) over 16 h. The reaction was flushed and the catalyst removed by filtration through Celite. The solvent was removed in vacuo and the resulting inhibitor purified by preparative HPLC (H_2O/AcCN) to afford compound **38** (43 mg, 42%). HPLC (system A: 99%, system B: 98%); MS (FAB) 929.5 (MH^+); HRMS calcd for $C_{46}H_{72}N_8O_{12}$ (MH^+) 929.53479, found: 929.53720.

General Procedure for Preparation of Inhibitors According to Scheme 1 (Methods A and C): Preparation of 34 (Method C). The HCl salt of **10b** after deprotection (where R3 = CH("*S*"-Me)Ph (77 mg, 0.24 mmol) was combined with the pentapeptide **2** (0.20 g, 0.22 mmol), TBTU (85 mg, 0.26 mmol), and diisopropylethylamine (0.13 mL, 0.73 mmol) in DMF (2.5 mL) at RT for 16 h. The reaction mixture was concentrated and the residue dissolved in EtOAc and washed sequentially with saturated aqueous $NaHCO_3$, 10% aqueous HCl, and brine before being dried ($MgSO_4$), filtered, and concentrated in vacuo. Purification (SiO_2, gradient 7:3 EtOAc/hexane to neat EtOAc) gave the precursor to **4** (R3 = CH("*S*"-Me)Ph) as a white solid (80 mg, 33%). This peptide (75 mg, 0.067 mmol) was treated with neat TFA (1.5 mL) for 1.5 h before being concentrated in vacuo. Purification by preparative HPLC gave compound **34** as a white solid (17 mg, 27%). HPLC (system A: 97%, system C: 95%); MS (FAB) 923.6 (MH^+); HRMS calcd for $C_{46}H_{66}N_8O_{12}$ (MH^+) 923.48785, found: 923.49097.

Compound 25 (Method C). Following method C (Scheme 1), the final compound was purified by preparative HPLC to give compound **25** as a white solid (85 mg, 73%). HPLC (system A: 98%, system C: 100%); MS (FAB) 819.3 (MH^+); HRMS calcd for $C_{38}H_{58}N_8O_{12}$ (MH^+) 819.42160, found: 819.42523.

Compound 26 (Method C). Following method C (Scheme 1), the final compound was purified by preparative HPLC to give compound **26** as a white solid (69 mg, 35%). HPLC (system A: 99%, system B: 97%); MS (FAB) 909.4 (MH^+); HRMS calcd for $C_{45}H_{64}N_8O_{12}$ (MH^+) 909.47217, found: 909.47500.

Compound 27 (Method B). Following method B (Scheme 1), the final compound was purified by preparative HPLC to give compound **27** as a white solid (17 mg, 19%). HPLC (system A: 100%, system C: 97%); MS (FAB) 953.0 (MH^+); HRMS calcd for $C_{46}H_{64}N_8O_{14}$ (MH^+) 953.46680, found: 953.46207.

Compound 28 (Method A). Following method A (Scheme 1), the final compound was purified by preparative HPLC to give compound **28** as a white solid (40 mg, 20%). HPLC (system A: 95%, system B: 96%); MS (FAB) 923.5 (MH^+); HRMS calcd for $C_{46}H_{66}N_8O_{12}$ (MH^+) 923.49100, found: 923.48785.

Compound 29 (Method A). Following method A (Scheme 1), the final compound was purified by preparative HPLC to give compound **29** as a white solid (4 mg, 2%). HPLC (system A: 99%, system C: 97%); MS (FAB) 923.5 (MH^+); HRMS calcd for $C_{46}H_{64}N_8O_{12}$ (MH^+) 921.472117, found: 921.46970.

Compound 30 (Method B). Following method B (Scheme 1), the final compound was purified by preparative HPLC to give compound **30** as a white solid (8 mg, 9%). HPLC (system A: 99%, system C: 95%); MS (FAB) 925.4 (MH^+); HRMS calcd for $C_{45}H_{64}N_8O_{11}S$ (MH^+) 925.44934, found: 925.44510.

Compound 31 (Method C). Following method C (Scheme 1), the final compound was purified by preparative HPLC to give compound **31** as a white solid (56 mg, 69%). HPLC (system A: 98%, system C: 97%); MS (FAB) 877.1 (MH^+).

Compound 32 (Method C). Following method C (Scheme 1), the final compound was purified by preparative HPLC to give compound **32** as a white solid (47 mg, 24%). HPLC (system A: 95%, system B: 97%); MS (FAB) 908.4 (MH^+); HRMS calcd for $C_{46}H_{65}N_7O_{12}$ (MH^+) 908.47693, found: 908.47693.

Compound 33 (Method C). Following method C (Scheme 1), the final compound was purified by preparative HPLC to give compound **33** as a white solid (27 mg, 13%). HPLC (system A: 99%, system C: 95%); MS (FAB) 923.6 (MH^+); HRMS calcd for $C_{46}H_{66}N_8O_{12}$ (MH^+) 923.48785, found: 923.49004.

Compound 35 (Method C). Following method C (Scheme 1), the final compound was purified by preparative HPLC to give compound **35** as a white solid (3 mg, 2%). HPLC (system A: 98%, system C: 98%); MS (FAB) 937.5 (MH^+); HRMS calcd for $C_{47}H_{68}N_8O_{12}$ (MH^+) 937.50398, found: 937.50630.

Compound 36 (Method A). Following method A (Scheme 1), the final compound was purified by preparative HPLC to give compound **36** as a white solid (75 mg, 78%). HPLC (system A: 99%, system C: 97%); MS (FAB) 921.3 (MH^+); HRMS calcd for $C_{46}H_{65}N_8O_{12}$ (MH^+) 921.47212, found: 921.46970.

Compound 37 (Method A). Following method A (Scheme 1), the final compound was purified by preparative HPLC to give compound 37 as a white solid (41 mg, 20%). HPLC (system A: 97%, system B: 97%); MS (FAB) 924.4 (MH^+); HRMS calcd for $C_{45}H_{65}N_9O_{12}$ (MH^+) 924.48309, found: 924.47820.

Compound 39 (Method B). Following method B (Scheme 1), the final compound was purified by preparative HPLC to give compound **39** as a white solid (7.5 mg, 6%). HPLC (system A: 98%, system C: 97%); MS (FAB) 915.5 (MH^+); HRMS calcd for $C_{41}H_{62}N_{12}O_{12}$ (MH^+) 915.47250, found: 915.46881.

Compound 40 (Method C). Following method C (Scheme 1), the final compound was purified by preparative HPLC to give compound **40** as a white solid (28 mg, 13%). HPLC (system A: 98%, system C: 98%); MS (FAB) 974.3 (MH^+); HRMS calcd for $C_{50}H_{68}N_8O_{12}$ (MH^+) 973.50398, found: 973.50580.

Compound 41 (Method B). Following method B (Scheme 1), the final compound was purified by preparative HPLC to give compound **41** as a white solid (7 mg, 7%). HPLC (system A: 98%, system C: 95%); MS (FAB) 1001.5 (MH^+) and 1003.5 $(MH+2)^+$.

Compound 42 (Method A). Following method A (Scheme 1), the final compound was purified by preparative HPLC to give compound **42** as a white solid (153 mg,39%). HPLC (system A: 100%, system B: 99%); MS (FAB) 895.4 (MH^+); HRMS calcd for $C_{44}H_{62}N_8O_{12}$ (MH^+) 895.45970, found: 895.45654.

Compound 43 (Method C). Following method C (Scheme 1), the final compound was purified by preparative HPLC to give 43 as a white solid (18 mg, 14%). HPLC (system A: 98%, system B: 97%); MS (FAB) 909.9 (MH^+); HRMS calcd for $C_{45}H_{64}N_8O_{12}$ (MH^+) 909.47217, found: 909.46860.

Compound 44 (Method C). Following method C (Scheme 1), the final compound was purified by preparative HPLC to give **44** as a white solid (15 mg, 8%). HPLC (system A: 97%, system B: 96%); MS (FAB) 937.5 (MH^+); HRMS calcd for $C_{47}H_{69}N_8O_{12}$ (MH^+) 937.50348, found: 937.50630.

Compound 45 (Method A). Following method A (Scheme 1), the final compound was purified by preparative HPLC to give 45 as a white solid (89 mg, 43%). HPLC (system A: 99%, system B: 100%); MS (FAB) 951.5 (MH^+); HRMS calcd for $C_{48}H_{70}N_8O_{12}$ (MH^+) 951.51917, found: 951.52110.

Compound 46 (Method A). Following method A (Scheme 1), the final compound was purified by preparative HPLC to give **46** as a white solid (9 mg, 8%). HPLC (system B: 95%, system C: 93%); MS (FAB) 951.1 (MH^+); HRMS calcd for $C_{48}H_{70}N_8O_{12}$ (MH^+) 951.51917, found: 951.52110.

Compound 47 (Method A). Following method A (Scheme 1), the final compound was purified by preparative HPLC to give **47** as a white solid (104 mg, 46%). HPLC (system A: 96%, system B: 99%); MS (FAB) 937.5 (MH^+); HRMS calcd for $C_{47}H_{68}N_8O_{12}$ (MH^+) 937.50348, found: 937.50730.

Compound 48 (Method A). Following method A (Scheme 1), the final compound was purified by preparative HPLC to give **48** as a white solid (100 mg, 48%). HPLC (system A: 95%, system C: 97%); MS (FAB) 951.4 (MH^+); HRMS calcd for $C_{48}H_{70}N_8O_{12}$ (MH^+) 951.51917, found: 951.52300.

Compound 49 (Method A). Following method A (Scheme 1), the final compound was purified by preparative HPLC to give **49** as a white solid (4 mg, 2%). HPLC (system A: 98%, system B: 91%); MS (electrospray) 961.4 $(M-H)^-$; HRMS calcd for $C_{45}H_{61}F_3N_8O_{12}$ (MH^+) 963.44391, found: 963.44740.

Biological Assays. The IC_{50} values were obtained from our in house protease assay which has been previously described and represent an average of at least four determinations.[7] The specificity of selected compounds was determined against a variety of serine proteases (human leukocyte and porcine pancreatic elastases (HLE and PPE), bovine pancreas α-chymotrypsin) and one cysteine protease (human liver cathepsin B) as described previously.[27b]

Expression and Purification of NS3 Protease. The NS3 protease domain was expressed in the pET29b vector (Novagen Inc.) and encoded a modified BK strain sequence that spanned amino acids 1−180 and contained a C-terminal solubilization motif (ASKKKK).[30] The expression and purification protocol was exactly as previously described.[32]

NMR Sample Preparation. NMR samples were prepared by adding 24 μL of concentrated solution of inhibitor **25** in DMSO-d_6 to an aqueous buffer composed of 50 mM Na_2PO_4, 300 mM NaCl, 3 mM dithiothreitol-d_{10} and 10% (v/v) D_2O (spiked with 3-(trimethylsilyl)-propionic 2,2,3,3-d_4) at pH 6.5. The final volume of these solutions was 600 μL with an inhibitor concentration ranging between 1.1 and 1.5 mM. To these samples was added a concentrated stock solution of NS3 protease (9.2 mg/mL, ∼450 μM) in a buffer identical to that described above such that an inhibitor/protease ratio of 30:1 to 35:1 was typically achieved. For the competition experiment, a stock solution of a potent activated carbonyl inhibitor (IC_{50} = 23.5 nM) in DMSO-d_6 (3.6 mM) was added to one of the samples described above such that a final inhibitor **25**/protease/potent inhibitor ratio of 34:1:4 was achieved.

NMR Methods. All spectra were acquired on a Bruker DRX 600 MHz NMR spectrometer equipped with a 5 mm TXI probe at 27 °C. Two-dimensional (2D) double quantum-filtered COSY (DQF−COSY), TOCSY, NOESY, and ROESY spectra were acquired using standard pulse sequences with time proportional phase incrementation (TPPI) method. Suppression of the solvent signal was achieved by the use of presaturation or by inserting a 3−9−19 WATERGATE module prior to data acquisition.[33] The 2D transferred-NOESY experiments were recorded with mixing time of 70, 100, 150, and 200 ms. In these experiments, a 25 ms spin-lock pulse was applied prior to t_1 delay in order to eliminate protein background signals.[34] The ROESY experiment was recorded with a 300 ms spin-lock period. The 2D data sets were typically acquired with 2048 points in t_2, 350−420 points in t_1 and 128 scans. The data were processed and analyzed using XWinNMR and WinNMR software (Bruker Canada, Milton, Ontario) and Felix software (Molecular Simulations Inc., San Diego, CA). Shifted sine-bell apodization and zero-filling (2048 × 1048 real points) were applied prior to Fourier transformation, and subsequent baseline corrections were applied in one or both dimensions.

Computational Methods. The NS3 bound conformation of inhibitor **25** was modeled by a simulating annealing protocol using Discover 95.0 and the CFF95 force field (Molecular Simulations Inc., San Diego, CA). The dynamics were performed without cross-terms and nonbonded cutoffs and with a dielectric constant of 1.0. A total of 60 NMR-derived distance restraints were generated from transferred-NOESY volume buildup rates using the Assign module of Felix software (Molecular Simulations Inc., San Diego, CA). These NMR distance restraints were applied as strong (1.8−2.5 Å), medium (1.8−3.5 Å), or weak (1.8−5.0 Å) flat-bottomed potentials having force constants of 15 kcal/mol·Å^2. Pseudoatoms defining

the centroids of the phenyl aromatic ring and the methyl groups were introduced in the definition of the NOE restraints, and the interproton distances were corrected accordingly.[35] A single, high temperature unrestrained dynamics run was performed at 900 K using a time step of 1 fs, with 50 structures collected at 1 ps intervals to generate a starting set of conformations. Each structure was then retrieved, cooled, and minimized using the following simulated annealing protocol. The temperature was initially lowered to 750 K at a rate of 30 K/ps where only strong restraints were applied. The remaining restraints were added, and additional cooling to first 500 K (25 K/ps) and then 300 K (20 K/ps) was performed, followed by restrained minimization (including cross-terms) to a final gradient of 0.005 kcal/mol·Å. A total of 14 low energy, NMR-consistent structures were isolated at the end of this protocol. These 14 structures were further divided into two subfamilies of structures (eight and six members, respectively) according to their slightly different P1 conformations. The first subfamily of structures (eight-members) was finally selected as the final representative set of NS3 bound conformations based on additional knowledge of the three-dimensional structure of the NS3 protease bound to an inhibitor (unpublished data). These final eight structures are shown superimposed (P1−P4 backbone atoms only) in Figure 2. The root-mean-square deviation for the backbone atoms of P1−P4 is 0.21 Å. None of these structures have distance violations greater than 0.2 Å and the average total restraint violation energy is 0.43 kcal/mol with a S. D. = 0.21 kcal/mol.

Supporting Information Available: ^{1}H NMR data. This material is available free of charge via the Internet at http://pubs.acs.org.

Acknowledgment. We gratefully acknowledge Colette Boucher and Sylvain Bordeleau for providing analytical support. We also thank Diane Thibeault, Roger Maurice, Pierre Bonneau, and Céline Plouffe for assay support in this study. Finally, we thank Paul Anderson, Daniel Lamarre, and Michael Cordingley for their encouragement and support.

References

(1) Hoofnagle, J. H.; Di Bisceglie, A. M. Drug Therapy: The Treatment of Chronic Viral Hepatitis C. *N. Engl. J. Med.* **1997**, *336*, 347−355.

(2) World Health Organization homepage: http://www.who.int, Fact Sheet No. 164, October 2000.

(3) For recent reviews, see: (a) Bartenschlager, R. The NS3/4A Proteinase of the Hepatitis C Virus: Unraveling Structure and Function of an Unusual Enzyme and a Prime Target for Antiviral Therapy. *J. Viral Hep.* **1999**, *6*, 165−181. (b) De Francesco, R.; Steinkühler, C. *Hepatitis C Viruses* **2000**, *242*, 149−169.

(4) (a) Lamarre, D.; Anderson, P.; Bailey, M.; Beaulieu, P.; Bolger, G.; Bonneau, P.; Bös, M.; Cameron, D.; Cartier, M.; Cordingley, M; Faucher, A.-M.; Goudreau, N.; Kawai, S.; Kukolj, G.; Lagacé, L.; LaPlante, S.; Narjes, H.; Poupart, M.-A.; Rancourt, J.; Sentjens, R.; St George, R.; Simoneau, B.; Steinmann, G.; Thibeault, D.; Tsantrizos, Y.; Weldon, S.; Yong, C.-L.; Llinàs-Brunet, M. An NS3 Protease Inhibitor with Antiviral Effects in Humans Infected with Hepatitis C Virus. *Nature* **2003**, *426*, 186−189. (b) Llinàs-Brunet, M.; Bailey, M.; Bolger, G.; Brochu, C.; Faucher, A.-M.; Ferland, J., Garneau, M.; Ghiro, E.; Gorys, V.; Grand-Maître, C.; Halmos, T.; Lapeyre-Paquette, N.; Liard, F.; Poirier, M.; Rhéaume, M.; Tsantrizos, Y.; Lamarre, D. Structure−Activity Study on a Novel Series of Macrocyclic Inhibitors of the Hepatitis C Virus NS3 Protease Leading to the Discovery of BILN 2061. *J. Med. Chem.* **2004**, *47*, 1605−1608.

(5) (a) Love, R. A.; Parge, H. E.; Wickersham, J. A.; Hostomsky, Z.; Habuka, N.; Moomaw, E. W.; Adachi, T.; Hostomska, Z. The Crystal Structure of Hepatitis C Virus NS3 Proteinase Reveals a Trypsin-like fold and a Structural Zinc Binding Site. *Cell* **1996**, *87*, 331−342. (b) Kim, J. L.; Morgenstern, K. A.; Lin, C.; Fox, T.; Dwyer, M. D.; Landro, J. A.; Chambers, S. P.; Markland, W.; Lepre, C. A.; O'Malley, E. T.; Harbeson, S. L.; Rice, C. M.; Murcko, M. A.; Caron, P. R.; Thomson, J. A. Crystal Structure of the Hepatitis C Virus NS3 Protease Domain Complexed with a Synthetic NS4A Cofactor Peptide. *Cell* **1996**, *87*, 343−355. (c) Yan, Y.; Li. Y.; Munshi, S.; Sardana, V.; Cole, J. L.; Sardana, M.; Steinkühler, C.; Tomei, L.; De Francesco, Kuo, L.; Chen, Z. Complex of NS3 Protease and NS4A Peptide of BK Strain Hepatitis C Virus: A 2.2A Resolution Structure in a Hexagonal Crystal Form. *Protein Sci.* **1998**, *7*, 837−847.

(6) (a) Grakoui, A.; Wychowski, C.; Lin, C.; Feinstone, S. M.; Rice, C. M. Expression and Identification of Hepatitis C Virus Polyprotein Cleavage Products. *J. Virol.* **1993**, *67*, 1385−1395. (b) Bartenschlager, R.; Ahlborn-Laake, L.; Mous, J.; Jacobsen, H. Nonstructural Protein 3 of the Hepatitis C Virus Encodes a Serine-type Proteinase required for Cleavage at the NS3/4 and NS4/5 Junctions. *J. Virol.* **1993**, *67*, 3835−3844. (c) Tomei, L.; Failla, C.; Santolini, E.; De Francesco, R.; La Monica, N. NS3 is a Serine Protease Required for Processing of Hepatitis C Virus Polyprotein. *J. Virol.* **1993**, *67*, 4017−4026. (d) Eckart, M. R.; Selby, M.; Masiarz, F.; Lee, C.; Berger, K.; Crawford, C.; Kuo, C.; Kuo, G.; Houghton, M.; Choo, Q.-L. Biochem. The Hepatitis C Virus Encodes a Serine Protease Involved in Processing of the Putative Nonstructural Proteins from the Viral Polyprotein Precursor. *Biophys. Res. Commun.* **1993**, *192*, 399−406. (e) Grakoui, A.; McCourt, D. W.; Wychowski, C.; Feinstone, S. M.; Rice, C. M. Characterization of the Hepatitis C Virus-encoded Serine Proteinase: Determination of Proteinase-dependent Polyprotein Cleavage Sites. *J. Virol.* **1993**, *67*, 2832−2843. (f) Kwong, A. D.; Kim, J. L.; Rao, G.; Liposvek, D.; Raybuck, S. A. Hepatitis C Virus NS3/4A Protease. *Antiviral Res.* **1998**, *40*, 1−18.

(7) (a) Bartenschlager, R.; Lohmann, V.; Wilkinson, T.; Koch, J. O. Complex Formation between the NS3 Serine-type Proteinase of the Hepatitis C Virus and NS4A and its Importance for Polyprotein Maturation. *J. Virol.* **1995**, *69*, 7519−7528. (b) Failla, C.; Tomei, L.; De Francesco, R. An Amino-terminal Domain of the Hepatitis C Virus NS3 Protease is Essential for Interaction with NS4A. *J. Virol.* **1995**, *69*, 1769−1777. (c) Lin, C.; Thomson, J. A.; Rice, C. M. A Central Region in the Hepatitis C Virus NS4A Protein allows Formation of an Active NS3−NS4A Serine Proteinase Complex in vivo and in vitro. *J. Virol.* **1995**, *69*, 4373−4380.

(8) Llinàs-Brunet, M.; Bailey, M.; Fazal, G.; Goulet, S.; Halmos, T.; Laplante, S.; Maurice, R.; Poirier, M.; Poupart, M.-A.; Thibeault, D.; Wernic, D.; Lamarre, D. Peptide-based Inhibitors of the Hepatitis C Virus Serine Protease. *Bioorg. Med. Chem. Lett.* **1998**, *8*, 1713−1718.

(9) Steinkühler, C.; Biasiol, G.; Brunetti, M.; Urbani, A.; Koch, U.; Cortese, R.; Pessi, A.; De Francesco, R. Product Inhibition of the Hepatitis C Virus NS3 Protease. *Biochemistry* **1998**, *37*, 8899−8905.

(10) Llinàs-Brunet, M.; Bailey, M.; Déziel, R.; Fazal, G.; Gorys, V.; Goulet, S.; Halmos, T.; Maurice, R.; Poirier, M.; Poupart, M.-A.; Rancourt, J.; Thibeault, D.; Wernic, D.; Lamarre, D. Studies on the C-terminal of Hexapeptide Inhibitors of the Hepatitis C Virus Serine Protease. *Bioorg. Med. Chem. Lett.* **1998**, *8*, 2719−2724.

(11) Llinàs-Brunet, M.; Bailey, M.; Fazal, G.; Ghiro, E.; Gorys, V.; Goulet, S.; Halmos, T.; Maurice, R.; Poirier, M.; Poupart, M.-A.; Rancourt, J.; Thibeault, D.; Wernic, D.; Lamarre, D. Highly potent and Selective Peptide-based Inhibitors of the Hepatitis C Virus Serine Protease: Towards Smaller Inhibitors. *Bioorg. Med. Chem. Lett.* **2000**, *10*, 2267−2270.

(12) Gante, J. Azapeptides. *Synthesis* **1989**, 405−413.

(13) Dutta, A. S.; Giles, M. Polypeptides. Part XIV. A Comparative Study of the Stability towards Enzymes of Model Tripeptides Containing α-Aza-amino acids, L.-Amino acids, and D-Amino acids. *J. Chem. Soc., Perkin Trans. 1* **1976**, 244−248.

(14) Dutta, A. S.; Giles, M.; Williams, J.; Inhibitors of Porcine Pancreatic Elastase. Peptides incorporating α-Aza-amino Acid Residues in the P_1 Position. *J. Chem. Soc., Perkin Trans. 1* **1986**, 1655−1663.

(15) (a) Powers, C.; Boone, R.; Carroll, D.; Gupton, B.; Kam, C.-M.; Nishio, N.; Sakamoto, M.; Tuhy, P. Reaction of Azapeptides with Human Leukocyte Elastase and Porcine Pancreatic Elastase. *J. Biol. Chem.* **1984**, *259*, 4288−4289. (b) Dorn, C.; Zimmerman, M.; Yang, S.; Yurewicz, E.; Ashe, B.; Frankshun, R.; Jones, H. Proteinase Inhibitors. Inhibitors of Elastase. *J. Med. Chem.* **1977**, *20*, 1464−1468.

(16) Dutta, A. S.; Giles, M.; Gormley, J.; Williams, J.; Kusner, E. Inhibitors of Human Leukocyte Elastase. Peptides Incorporating an α-Azanorvaline Residue or a Thiomethylene Linkage in Place of a Peptide Bond. *J. Chem. Soc., Perkin Trans. 1* **1987**, 111−120.

(17) Gassman, J.; Magrath, J. An Active-Site Titrant for Chymotrypsin, and Evidence that Azapeptide Ester are less Susceptible to Nucleophilic Attack than Ordinary Esters. *Bioorg., Med. Chem. Lett.* **1996**, *6*, 1771−1774.

(18) Gupton, B. F.; Carroll, D.; Tuhy, P.; C−M. Kam,; Power, J. C. Reaction of Azapeptides with Chymotrypsin-like Enzymes. *J. Biol. Chem*. **1984**, *259*, 4279−4287.
(19) Llinàs-Brunet, M.; Bailey, M. D.; Halmos, T.; Poupart, M. A.; Tsantrizos, Y. World (PCT) Patent WO9907734, 1999. Also presented by Halmos, T., Bailey M. D., Llinàs-Brunet, M., Goudreau, N. M., Lescop, E., The 16th American Peptide Symposium, Minnesota, MN, June 26-July 1, 1999, P625.
(20) Zhang, R.; Durkin, J. P.; Windsor, W. T. Azapeptides as Inhibitors of the Hepatitis C Virus NS3 Serine Protease. *Bioorg., Med. Chem. Lett.* **2002**, *12*, 1005−1008. Zhang, R. Azapeptides Useful in the Treatment of Hepatitis C. World (PCT) Patent WO 158929, 2001.
(21) For a review concerning approaches, see Dymock, B. W.; Jones, P. S.; Wilson, F. X. Novel Approaches to the Treatment of Hepatitis C Virus Infection. *Antiviral Chem. Chemother.* **2000**, *11*, 70−96.
(22) Sieber, P. Der 2-trimethylsilyläthyl-rest als Selektiv Abspaltbare Carboxy schutzgruppe. *Helv. Chim. Acta* **1977**, *60*, 2711−2716.
(23) André, F.; Boussard, G.; Bayeul, D.; Didierjean, C.; Aubry, A.; Marraud, M. Azapeptides. III. Experimental Structural Analysis of Aza-alanine and Aza-asparagine containing Peptides. *J. Pept. Res.* **1997**, *49*, 556−562.
(24) Powers, J. C.; Carroll, D.; Tuhy, P. Synthetic Active Site-directed Inhibitors of Elastolytic Protease. *Ann. N. Y. Acad. Sci*. **1975**, *256*, 420.
(25) Benatalah, Z.; Aubry, A.; Boussard, G.; Marraud, M. Evidence for a β-turn in an Azadipeptide Sequence. *Int. J. Pept. Protein Res.* **1991**, *38*, 603−605.
(26) Gray, C. J.; Ireson, J.; Parker, R. Preparation and Properties of some α-Aza-Amino acid Derivatives, Their Possible use in Peptide Synthesis. *Tetrahedron* **1977**, *33*, 739−743.
(27) (a) Jones, J. B.; Occhiato, E. Probing enzyme stereospecificity. Inhibition of α-Chymotrypsin and subtilisin Carlsberg by Chiral Amine- and Amino alcohol Derivatives. *Tetrahedron* **1996**, *52*, 4199−4214. (b) Ogilvie, W.; Bailey, M.; Poupart, M.-A.; Abraham, A.; Bhavsar, A.; Bonneau, P.; Bordeleau, J.; Bousquet, Y.; Chabot, C.; Duceppe, J.-S.; Fazal, G.; Goulet, S.; Grand-Maître, C.; Guse, I.; Halmos, T.; Lavallée, P.; Leach, M.; Malenfant, E.; O'Meara, J.; Plante, R.; Plouffe, C.; Poirier, M.; Soucy, F.; Yoakim, C.; Déziel, R. Peptidomimetic Inhibitors of the Human Cyto- megalovirus Protease. *J. Med. Chem*. **1997**, *40*, 4113−4135. (c) Chen, S.-H.; Lamar, J.; Victor, F.; Synder, N.; Johnson, R.; Heinz, B.; Wakulchik, M.; Wang, Q. Synthesis and Evaluation of Tripeptidyl α-ketoamides as Human Rhinovirus 3C Protease Inhibitors. *Bioorg., Med. Chem. Lett*. **2003**, *13*, 3531−3536.
(28) LaPlante, S.; Cameron, D.; Aubry, N.; Lefebvre, S.; Kukolj, G.; Maurice, R.; Thibeault, D.; Lamarre, D.; Llinàs-Brunet, M. Solution Structure of Substrate-based Ligands When Bound to Hepatitis C Virus NS3 Protease Domain. *J. Biol. Chem*. **1999**, *274*, 18618−18624.
(29) Ni, F. Recent developments in transferred NOE methods. *Prog. Nucl. Magn. Reson. Spectrosc.* **1994**, *26*, 517−606.
(30) LaPlante, S. R.; Aubry, N.; Bonneau, P. R.; Kukolj, G.; Lamarre, D.; Lefebvre, S.; Li, H.; Llinàs-Brunet, M.; Plouffe, C.; Cameron, D. R. NMR Line-broadening and Transferred NOESY as a Medicinal Chemistry Tool for Studying Inhibitors of the Hepatitis C Virus NS3 Protease Domain. *Bioorg., Med. Chem. Lett.* **2000**, *10*, 2271−2274.
(31) Steinkühler, C.; Biasiol, G.; Brunetti, M.; Urbani, A.; Koch, U.; Cortese, R.; Pessi, A.; De Francesco, R. Product Inhibition of the Hepatitis C Virus NS3. *Biochemistry* **1998**, *37*, 8899−8905.
(32) Goudreau, N.; Cameron, D. C.; Bonneau, P.; Gorys, V.; Plouffe, C.; Poirier, M.; Lamarre, D.; Llinàs-Brunet, M. NMR Structural Characterization of Peptide Inhibitors Bound to the Hepatitis C Virus NS3 Protease: Design of a New P2 Substituent. *J. Med. Chem*. **2004**, *47*, 123−132.
(33) Sklenar, V.; Piotto, M.; Leppik, R.; Saudek, V. Gradient-tailored Water Suppression for ^{1}H-^{15}N HSQC Experiments Optimized to Retain Full Sensitivity. *J. Magn. Reson. A* **1993**, *102*, 241−245.
(34) Scherf, T.; Anglister, J. A $T_{1\rho}$-filtered Two-dimensional Transferred NOE Spectrum for Studying Antibody Interactions with Peptide Antigens. *Biophys. J.* **1993**, *64*, 754−761.
(35) Wüthrich, K.; Billeter, M.; Braun, W. Pseudostructures for the 20 Common Amino Acids for use in Studies of Protein Conformations by Measurements of Intramolecular Proton−proton Distance Constraints with Nuclear Magnetic Resonance-filtered Two-dimensional Transferred NOE Spectrum for Studying Antibody Interactions with Peptide Antigens. *J. Biol. Mol.* **1983**, *169*, 949−961.

JM049864B